
# A coumarin based Schiff base probe for selective fluorescence detection of $Al^{3+}$ and its application in live cell imaging

Bhaskar Sen, Sanjoy Kumar Sheet, Romita Thounaojam, Ramen Jamatia, Amarta Kumar Pal, Kripamoy Aguan, Snehadrinarayan Khatua

PII: S1386-1425(16)30586-8
DOI: doi:10.1016/j.saa.2016.10.005
Reference: SAA 14704

To appear in:

Received date: 9 June 2016
Revised date: 15 September 2016
Accepted date: 8 October 2016

Please cite this article as: Bhaskar Sen, Sanjoy Kumar Sheet, Romita Thounaojam, Ramen Jamatia, Amarta Kumar Pal, Kripamoy Aguan, Snehadrinarayan Khatua, A coumarin based Schiff base probe for selective fluorescence detection of $Al^{3+}$ and its application in live cell imaging, (2016), doi:10.1016/j.saa.2016.10.005

# A Coumarin Based Schiff Base Probe for Selective Fluorescence Detection of $Al^{3+}$ and its Application in Live Cell Imaging

Bhaskar Sen,[a] Sanjoy Kumar Sheet,[a] Romita Thounaojam,[b] Ramen Jamatia,[a] Amarta Kumar. Pal,[a] Kripamoy Aguan[b] and Snehadrinarayan Khatua[a,*]

[a] *Centre for Advanced Studies, Department of Chemistry, North Eastern Hill University, Shillong, Meghalaya 793022, India.*
[b] *Department of Biotechnology and Bioinformatics, North Eastern Hill University, Shillong, Meghalaya 793022, India.*

Keywords: Coumarin, Schiff Base, Fluorescence, $Al^{3+}$ Sensing, Bio-imaging

**ABSTRACT:**

A new coumarin based Schiff base compound, **CSB-1** has been synthesized to detect metal ion based on the chelation enhanced fluorescence (CHEF). The cation binding properties of **CSB-1** was thoroughly examined in UV-vis and fluorescence spectroscopy. In fluorescence spectroscopy the compound showed high selectivity toward $Al^{3+}$ ion and the $Al^{3+}$ can be quantified in mixed aqueous buffer solution (MeOH: 0.01M HEPES Buffer; 9:1; v/v) at pH 7.4 as well as in BSA media. The fluorescence intensity of **CSB-1** was enhanced by ~ 24 fold after addition of only five equivalents of $Al^{3+}$. The fluorescence titration of **CSB-1** with $Al^{3+}$ in mixed aqueous buffer afforded a binding constant, $K_a = (1.06 \pm 0.2) \times 10^4\ M^{-1}$. The colour change from light yellow to colourless and the appearance of blue fluorescence, which can be observed by the naked eye, provides a real-time method for $Al^{3+}$ sensing. Further the live cell imaging study indicated that the detection of intracellular $Al^{3+}$ ions are also readily possible in living cell.

* Corresponding author. Tel.: +91-364-272-2636; e-mail: snehadri@gmail.com; skhatua@nehu.ac.in

## 1. Introduction

The rational design and synthesis of fluorescent chemosensors for the selective detection and quantification of specific cation, anion, ion-pair and biomolecule has attracted considerable interest due to their importance in environmental and biological applications [1-11]. Highly selective metal ions sensing and live cell imaging in chemistry and chemical biology is an extremely interesting and important area of current research [12-16]. Aluminum as the third most abundant metallic element in the lithosphere was found to be neurotoxic to living organism. $Al^{3+}$ ion widely exists in the environment, normally in natural waters and in most plants and can enter the human body through foods and water [17-19]. High concentrations of $Al^{3+}$ are toxic to plants, vegetables, fish, algae, bacteria, and other species in aquatic environment [20-22]. The excessive exposure of $Al^{3+}$ to human body is harmful as the $Al^{3+}$ toxicity is believed to be one of the main causes of neurological disorders such as Alzheimer's disease, Parkinson's disease, amyotrophic lateral sclerosis (ALS), chronic renal failure, bone softening and gastrointestinal problems etc. [23-24]. Accordingly, the development of $Al^{3+}$-specific molecular probes have been of considerable interest in the biological and analytical chemical sciences [25-30]. The detection and quantification of $Al^{3+}$ has been problematic because of the strong hydration of $Al^{3+}$ in aqueous media which leads to its weak coordination ability in comparison to transition metals [31-35]. Therefore, it is challenging to design a highly selective and sensitive fluorescence probe for $Al^{3+}$ in aqueous media as the other interfering ions such as $Zn^{2+}$, $Cu^{2+}$, $Cd^{2+}$, $Hg^{2+}$ and $Pb^{2+}$ are very much present in biological system and in environmental sample. [36-38]. Due to the hard nature, $Al^{3+}$ prefers to bind N and O donor ligands and, therefore, most of the reported $Al^{3+}$ probes are based on the N and O donor ligand [39-42].

.

Schiff base derivatives having N and O donor site and a fluorescent moiety are appealing tools for designing optical probes for metal ions [43-46]. It is already established that Schiff base alone is weekly or non-fluorescent as the fluorescence is quenched due to the free rotation around C=N bond [47]. In the recent past, numerous research papers described the specific detection of various metal ions through the chelation of Schiff base probes which obstruct the above C=N isomerization mechanism [47-49]. Coumarin is a well-known chromophore used in fluorescence sensing of cation, anion and bio-relevant species [50-54]. Coumarin derivatives have been used extensively due to their tunable photophysical properties and substantial fluorescent behavior in the visible region. The coumarin derived Schiff base probe containing an O or N donor can bind the metal ion as well as act as a signaling unit.

Herein, we report the synthesis and characterization of coumarin based Schiff base, **CSB-1** and the $Al^{3+}$ ion sensing in mixed aqueous buffer as well as BSA media through the chelation enhanced fluorescence (CHEF). Further, the imaging experiments using live HeLa cell and detection of intracellular $Al^{3+}$ ion in living cell are also discussed herein.

## 2. Experimental

### *2.1 Materials and methods*

All commercially available chemicals were used without further purification except 3-Amino-4-hydroxycoumarin which was synthesized according to the reported procedure [55]. The IR spectra were measured on a Perkin-Elmer FT- IR spectrometer with KBr pellets in the range of 4000–400 $cm^{-1}$. Nuclear magnetic resonance spectra were recorded on Bruker Avance II (400MHz) spectrometer using the residual protic solvent resonance as the internal standard and chemical shifts were expressed in ppm. ESI-MS was performed with Waters ZQ-4000 and QTOF Micro YA 263 mass

spectrometer. Elemental analysis was carried out in PerkinElmer 2500 series II elemental analyzer. The UV–vis absorption spectra were recorded using a Perkin-Elmer Lambda 25 UV–vis scanning spectrophotometer. Fluorescence spectra were obtained with a Hitachi F-4500 spectrophotometer with quartz cuvette (path length = 1 cm).

### *2.2 A general method for the UV-vis and fluorescence experiments*

The different metal ions sensing by coumarin Schiff base compound, **CSB-1** was investigated using UV–vis and fluorescence spectrophotometer in mixed aqueous buffer (MeOH : 0.01 M HEPES, 9:1 v/v, 7.4 pH) solution at room temperature. A stock solution of **CSB-1** (1 mM) was prepared in methanol and diluted to 10 μM and 50 μM using 0.01M HEPES buffer and methanol for $Al^{3+}$ sensing in fluorescence and UV-vis spectroscopy, respectively. Stock solutions of various cations (10 mM) were prepared using their perchlorate salt in Millipore water. An excitation wavelength at $\lambda$ = 395 nm was used for all fluorescence experiments and the excitation and the emission slits were set to 2.5 mm.

### *2.3 Binding constant calculation*

The binding constant of the metal complex formed in solution has been estimated by using the standard Benesi-Hildebrand (B-H) equation 1.

$$1/(I - I_0) = 1/\{K_a(I_{max} - I_0)C\} + 1/(I_{max} - I_0) \qquad (1)$$

$I_0$ is the fluorescence intensity of free **CSB-1** at emission maximum ($\lambda_{em}$ = 461 nm), I is the observed fluorescence intensity at that particular wavelength in the presence of a certain concentration of the metal ion (C), $I_{max}$ is the maximum fluorescence intensity value that was obtained at $\lambda_{em}$ = 461 nm during titration with varying metal ion concentration, $K_a$ is the

binding constant and was determined from the slope of the linear plot, and C is the concentration of the $Al^{3+}$ ion added during titration experiment.

### *2.4 Quantum Yield calculation*

The fluorescence quantum yield was determined using fluorescein as reference with a known $\Phi_R$ of 0.91 in 0.1M NaOH [56]. The compounds (free **CSB-1** and in the presence of $Al^{3+}$) and reference were excited in such a way that the absorbance should nearly equal (~0.1). The quantum yield is calculated according to the following equation:

$$\Phi_S = \Phi_R \times (1\text{-}10^{-A_R})/(1\text{-}10^{-A_S}) \times I_S/I_R \times \eta_S^2/\eta_R^2 \qquad (2)$$

Here, $\Phi_S$ and $\Phi_R$ are the fluorescence quantum yield of the sample and reference, respectively. $I_S$ and $I_R$ are the area under emission spectra of the sample and the reference, respectively. $A_S$ and $A_R$ are the absorbance of the sample and the reference solution at the excitation wavelength, respectively. $\eta_S$ and $\eta_R$ are the values of refractive index for the respective solvent used for the sample and reference.

### *2.5 Determination of detection limit*

The limit of detection (DL) of **CSB-1** for $Al^{3+}$ was calculated based on the fluorescence titration data and determined from the following equation:

$$DL = 3\sigma/K \qquad (3)$$

Where $\sigma$ is the standard deviation of the blank solution; $K$ is the slope of the calibration curve.

### *2.6 Methods for cell imaging*

A fluorescence Inverted microscope (Leica DMI4000B) was used to visualize the fluorescence of the cells following the addition of the respective compound with 20X

objective lens. Fluorescence detection was carried out using excitation filter BP 340-380 for complex **CSB-1**. The HeLa cells were cultured in DMEM media containing low glucose (Invitrogen) with 10% FBS (Invitrogen) at 37°C in 5% $CO_2$ incubator chamber. For imaging experiments, cells were seeded into 6 well plates. Cells were washed with PBS (phosphate buffer saline) after 24 hours of incubation and fresh 500 μL of PBS were added in two successive wells. One of the well was treated with only **CSB-1** (10 μM) and incubated for 20 min. Other well was initially treated with $Al^{3+}$ (30 μM) and incubated for 10 min. After incubation, the cells were washed with PBS buffer, treated with **CSB-1** (10 μM) and incubated for another 10 min. After incubation, both the $Al^{3+}$ treated and untreated cells were washed with PBS buffer twice and observed under fluorescence microscope at bright field and blue emission channel at excitation of 340-380 nm.

### *2.7 Theoretical study*

The electronic properties of the **CSB-1** and $Al^{3+}$**-CSB-1** complex has been investigated by means of density functional theory (DFT) calculations. All calculations have been performed using the B3LYP exchange correlation functional [57-59] as implemented in the *Gaussian 03*(G03) program package. The 6-31G+ (d, p) basis set was assigned for the elements.

### *2.8 Synthesis of CSB-1[(E)-3-(2-hydroxybenzylideneamino)-4-hydroxy-2H-chromen-2-one]*

Compound **CSB-1** was synthesized by an extremely facile procedure as illustrated in Scheme 1. The solution (10 ml) of salicylaldehyde (0.049 ml, 0.455 mmol) in methanol was added dropwise to the solution (20 ml) of 3-amino-4-hydroxycoumarin (75.0 mg, 0.423 mmol) in methanol over a period of 15 minutes with continuous stirring. The solution was stirred at room temperature. The pH of the solution was maintained at ~8.0 by the drop wise addition of dilute methanolic NaOH solution. The solution turned into yellow after few

minutes which indicated the formation of the intended product. The stirring was continued further for 12 h and the volume of the solution was reduced under rotary evaporator. A yellow solid compound was obtained and washed thoroughly with chloroform and diethyl ether to remove unreacted excess salicylaldehyde. Finally it was dried under vacuum to get solid yellow **CSB-1**. Yield: 115 mg (96 %). $^{1}$H NMR (DMSO-$d_6$, 400 MHz,): $\delta$(ppm) = 15.66 (s, 1H, O-$H_{coumarin}$), 9.97 (s, $H_{11}$), 7.91 (d, $^{3}J$ = 8.0 Hz, 1H), 7.43 (t, $^{3}J$ = 8.0 Hz, 1H), 7.25 (d, $^{3}J$ = 8.0, 1H), 7.20-7.10 (m, 3H), 6.76-6.74 (m, 2H). $^{13}$C NMR (DMSO-$d_6$, 100 MHz): $\delta$(ppm) = 169.9, 161.1, 161.0, 152.6, 151.2, 130.4, 129.6, 129.3, 125.0, 123.5, 122.2, 121.3, 117.2, 116.6, 115.6, 107.2. ESI-MS $[C_{16}H_{11}NO_4 + H]^+$: calcd., *m/z* = 282.07; found *m/z*, 282.05 and ESI-MS $[C_{16}H_{11}NO_4 + Na^+]$: calcd., *m/z* = 304.06; found, *m/z* = 304.13. C, H, N analysis: Calcd. (%) for $C_{16}H_{11}NO_4$ (*Mw* = 281.07 g $mol^{-1}$): C 68.32, H 3.94, and N 4.98; found: C 68.31, H 3.96, and N 4.99. FTIR (KBr disk) ($\nu_{max}$ /$cm^{-1}$): 3435, 1664, 1611, 1537, 1464, 1417, 1363, 1203, 1144, 1085, 751, 728, 468.

## 3. Results and discussion

The coumarin based Schiff base compounds, **CSB-1** was synthesized by reacting salicylaldehyde and 3-amino-4-hydroxycoumarin in methanol and isolated as a bright yellow solid with a high yield (Scheme 1). The **CSB-1** was fully characterized by elemental analysis, $^{1}$H and $^{13}$C NMR spectroscopy and ESI-MS spectrometry. The photophysical properties were determined by UV-vis and fluorescence spectroscopy. The $^{1}$H and $^{13}$C spectra of **CSB-1** recorded in DMSO-$d_6$ at room temperature clearly showed all expected resonances for the Schiff base probe (Figure S1, S2 in SI). For **CSB-1**, the ESI-MS clearly displayed peaks at *m/z* = 282.05 (calcd. 282.07) and 304.13 (calcd. 304.06) that are assigned to $[C_{16}H_{11}NO_4 + H^+]$ and $[C_{16}H_{11}NO_4 + Na^+]$, respectively (Figure S3 in SI).

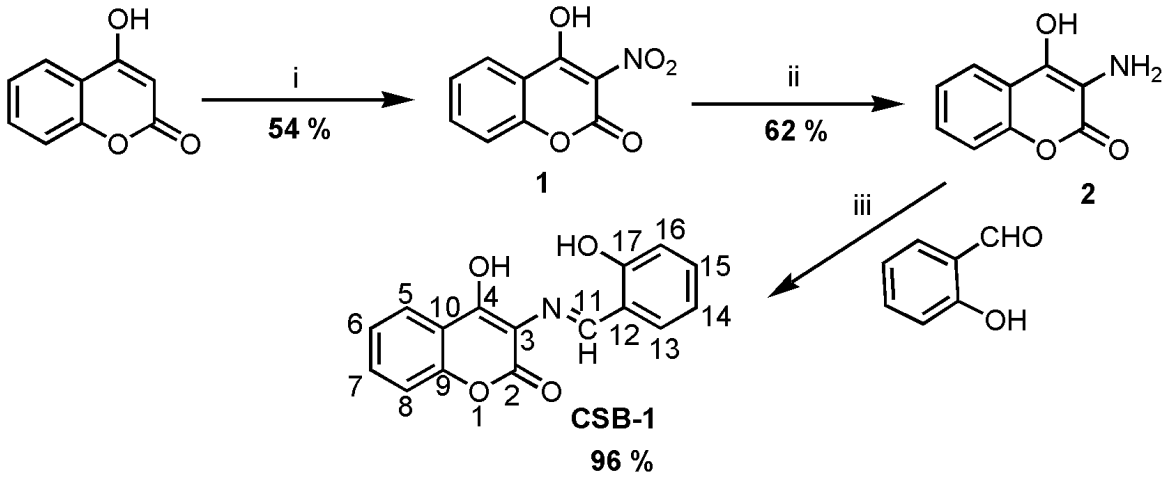


**Scheme 1**: Synthesis of probe, **CSB-1**. Reagents and conditions: (i) Glacial acetic acid, conc. $HNO_3$, stirring, 100 °C, 15 min. (ii) 5% Pd/C, 1% HCl in MeOH, $H_2$, 5h. (iii) MeOH, NaOH solution, pH ~8.0, stirring, 12h. Compound **1** and **2** were synthesized according to the reported published procedure [55].

### *3.1 Sensing study in UV-vis and fluorescence spectroscopic channel*

The UV-vis spectrum of **CSB-1** in mixed aqueous buffer (0.01M HEPES buffer : methanol 1:9 ; v/v; pH 7.4) at room temperature displayed bands at 326 nm ($\varepsilon$ = 9900 $M^{-1}$ $cm^{-1}$), 339 nm ($\varepsilon$ = 11000 $M^{-1}$ $cm^{-1}$), 395 nm ($\varepsilon$ = 11000 $M^{-1}$ $cm^{-1}$), 415 nm ($\varepsilon$ = 10000 $M^{-1}$ $cm^{-1}$) and 455 nm ($\varepsilon$ = 4500 $M^{-1}$ $cm^{-1}$), assigned to intraligand (IL) $\pi$-$\pi^*$ and n-$\pi^*$ transitions. The effect of the different cations (present as perchlorate salts) was examined in a mixed aqueous buffer (0.01M HEPES buffer: methanol 1:9 v/v; pH 7.4) at room temperature. As shown in figure 1a, metal ions *e.g.* $Na^+$ , $K^+$, $Ca^{2+}$, $Ag^+$, $Fe^{3+}$, $H^+$ and $Hg^{2+}$ did not show any response whereas other metals ions *e.g.* $Cu^{2+}$, $Ni^{2+}$, $Co^{2+}$, $Mn^{2+}$, $Zn^{2+}$, $Cd^{2+}$, $Pb^{2+}$, $Cr^{3+}$ and $Al^{3+}$ altered the n-$\pi^*$ transition band. The addition of $Al^{3+}$ caused a decrease in the absorbance of the peak at 455 nm along with the growth of two peaks at 395 nm and 415 nm (Figure 1b). The decrease and increase in absorbance at 455 nm, 395 nm and 415 nm indicate chelation of $Al^{3+}$. But other

cations also altered the n-π* transition band remarkably. Therefore, the UV-vis spectroscopic channel is not beneficial to sense $Al^{3+}$ selectively.

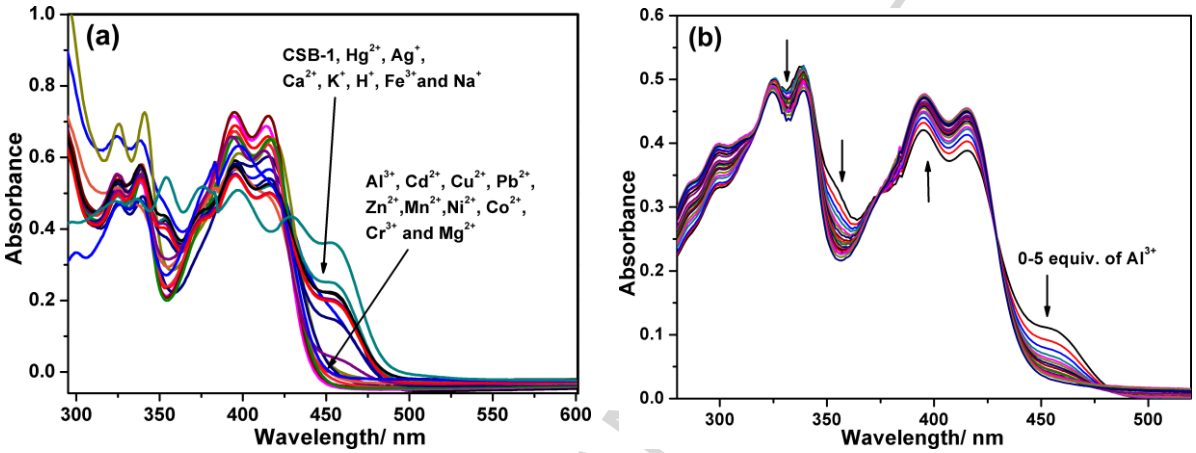


**Figure 1:** (a) UV−vis absorption spectra of **CSB-1**(50 μM) with various cations in mixed aqueous buffer (0.01M HEPES buffer: methanol 1:9; v/v; pH 7.4) at room temperature. (b) Absorption titration of **CSB-1** (50 μM) with $Al^{3+}$ (0-300 μM) in mixed aqueous buffer at pH 7.4.

The compound **CSB-1** itself is weakly fluorescent under neutral aqueous conditions (0.01M HEPES buffer: methanol 1:9; v/v; pH 7.4) at room temperature. It exhibits very weak fluorescence ($\Phi$ = 0.026) at $\lambda_{em}$ = 461 nm when excited at $\lambda_{ex}$ = 395 nm. The weak fluorescence of **CSB-1** is due to the C=N isomerization with the 2-hydroxybenzylidene amino group (Scheme 2) [60-61]. Upon addition of only 5 equiv. of $Al^{3+}$ to mixed aqueous buffer solution of **CSB-1**, however, a significant enhancement of the emission was documented at 461 nm ($\Phi$ = 0.731). The bright blue luminescence may readily be observed by the naked eye using a hand-held UV light (Figure 2a inset). The fluorescence intensity was not notably influenced by the addition of other competitive metal ions, such as $Na^{+}$, $K^{+}$, $Ca^{2+}$, $Ag^{+}$, $Cu^{2+}$, $Ni^{2+}$, $Co^{2+}$, $Mn^{2+}$, $Zn^{2+}$, $Cd^{2+}$, $Hg^{2+}$, $Mg^{2+}$, $H^{+}$, $Fe^{3+}$, $Cr^{3+}$ and $Pb^{2+}$. It is assumed that the coordination of the $Al^{3+}$ ion to the O and N center of the **CSB-1**, the C=N isomerization with the 2-hydroxybenzylidene amino group is inhibited and as a consequence

the fluorescence is enhanced (Scheme 2). The fluorescence titration of **CSB-1** (10 μM) with 0-6.0 equiv. of $Al^{3+}$ shows a gradual red shift and a 24-fold enhancement of the initially weak fluorescence band at $\lambda_{max}$ 453 to 461 nm (Figure 2b).The Benesi-Hilderbrand (B-H) plot shows a linear fitting and confirms the 1:1 stoichiometry of $Al^{3+}$ to **CSB-1** (Figure 3a).

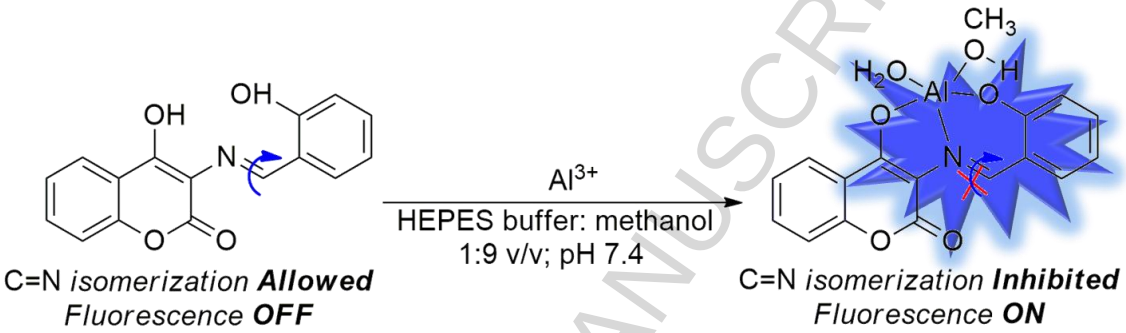


**Scheme 2:** Schematic illustration of $Al^{3+}$ sensing by inhibiting of C=N isomerization.

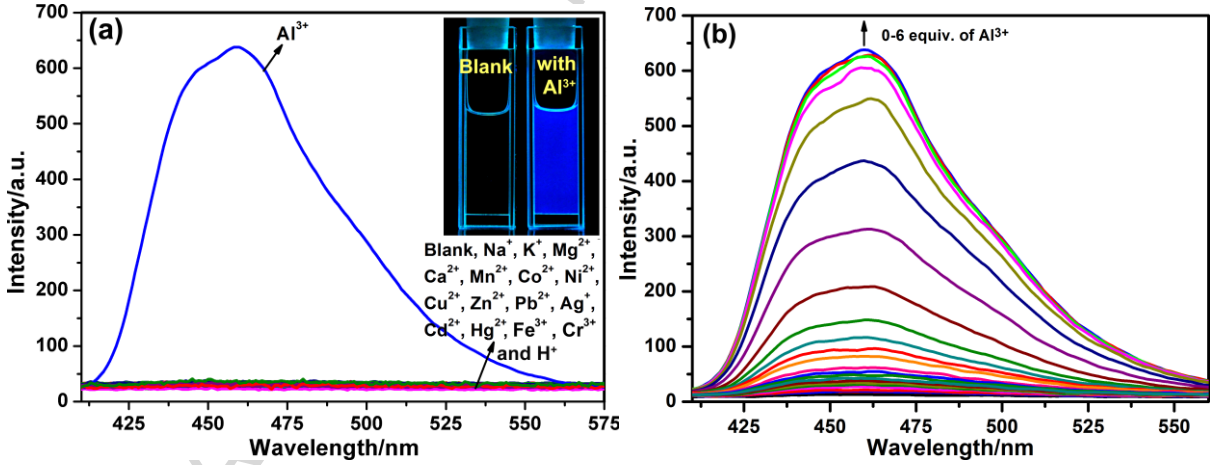


**Figure 2:** (a) Cation selectivity by **CSB-1** (10 μM) in fluorescence spectroscopic channel in aqueous buffer (0.01M HEPES buffer: methanol 1:9; v/v; pH 7.4) at room temperature.(*inset)* Naked eye fluorescence colour change of **CSB-1** in addition of $Al^{3+}$. (b) Fluorescence titration of **CSB-1** (10 μM) with $Al^{3+}$ (0-60 μM) in aqueous buffer at pH 7.4.

The B-H plot from the fluorescence titration of **CSB-1** with $Al^{3+}$ in mixed aqueous buffer afforded a binding constant, $K_a$ = (1.06 ± 0.2) × $10^4$ $M^{-1}$. During the fluorescence titration the emission intensity of **CSB-1** is linearly increased at a lower concentration of $Al^{3+}$ and the calculated detection limit of $Al^{3+}$ was as low as 1.34 μM (Figure S4 in SI) in a mixed aqueous

buffer solution which is lower than many other reported $Al^{3+}$ probes and the maximum permissible level stipulated by WHO (7.41 μM) [62-67]. A competition experiments with other metal ions were carried out with the fluorescence spectroscopy to check for possible interferences in $Al^{3+}$ sensing. The addition of other competitive metal ions (100 equiv.) to **CSB-1** (10 μM) did not influence the fluorescence intensity. Consequently, $Al^{3+}$ (5 equiv.) in a 1:100 mixture of **CSB-1** and other competitive cations was readily detected by a clear fluorescence enhancement at 461 nm (Figure 3b). However, the $Al^{3+}$ sensing was slightly interfered by $Fe^{3+}$ and $Cr^{3+}$ ions.

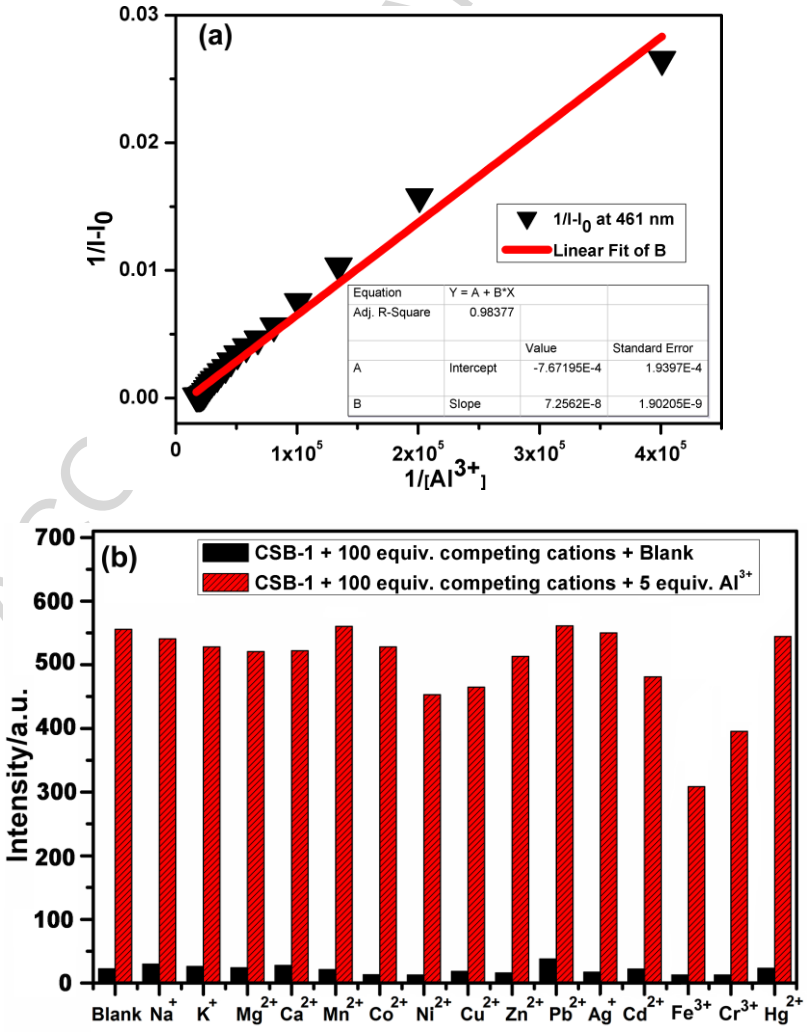


**Figure 3.** (a) Benesi-Hildebrand (B-H) plot from the fluorescence titration of **CSB-1** with $Al^{3+}$ (b) Selectivity studies of **CSB-1 (50 μM)** with $Al^{3+}$ (5 equiv.) in the presence of competing cations (100 equiv.) in mixed aqueous buffer solution.

### *3.1.1. Effect of pH in $Al^{3+}$ detection and reversibility study*

The effect of the pH in $Al^{3+}$ detection was examined in fluorescence spectroscopy. The **CSB-1** shows weak fluorescence over the pH range of 3.0-11.0 (Figure 4). On the other hand, upon the addition of only 2.0 equiv. of $Al^{3+}$, a significant increase in the fluorescence intensity is observed in the pH range of 7.0–11.0, and this endorses its possibility for $Al^{3+}$ detection under physiological conditions (Figure 4).

It has been already established that pyrophosphates (PPi) and EDTA can form stable complexes with $Al^{3+}$ [68-69]. To check the stability of the $Al^{3+}$**-CSB-1** complex, PPi / EDTA was used to remove $Al^{3+}$ from the $Al^{3+}$**-CSB-1** complex. When incremental amount of PPi or EDTA was added to the $Al^{3+}$**-CSB-1** ensemble solution, the intensity of the emission band at 461 nm was decreased very slowly. The emission intensity was decreased by ~ 8 fold after addition of 87.5 equiv. of PPi (Figure S5). In a separate titration experiment, the emission intensity was decreased by ~ 3.6 fold after addition of 880 equiv. of EDTA (Figure S6). Therefore, the $Al^{3+}$**-CSB-1** complex is very stable and the $Al^{3+}$ displacement by PPi / EDTA is inefficient.

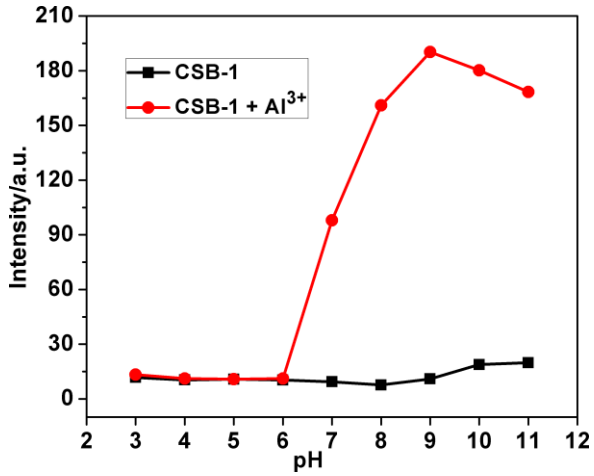


**Figure 4.** The pH effect on fluorescence responses of **CSB-1** (10 μM) in the absence (black) and presence (red) of $Al^{3+}$ (5 equiv.). Excitation and emission was monitored at λ = 395 nm and 461 nm respectively.

### *3.1.2. Detection of $Al^{3+}$ in BSA media*

Bovine serum albumin (BSA) is a hydrophobic protein and it contains specific metal ion binding sites. For the practical applicability of the probe, **CSB-1** and to detect and quantify $Al^{3+}$ ions in the biological medium we examined the photophysical properties of the probe in the presence of bovine serum albumin (BSA). The **CSB-1** is weakly fluorescent in BSA media as well as in the mixed HEPES buffer. The fluorescence intensity of the **CSB-1** at 469 nm is enhanced by ~12 fold upon addition of 5 equiv. of $Al^{3+}$ and the band is blue shifted to 459 nm in BSA medium (Figure 5a). Whereas, in the mixed HEPES buffer media the fluorescence intensity

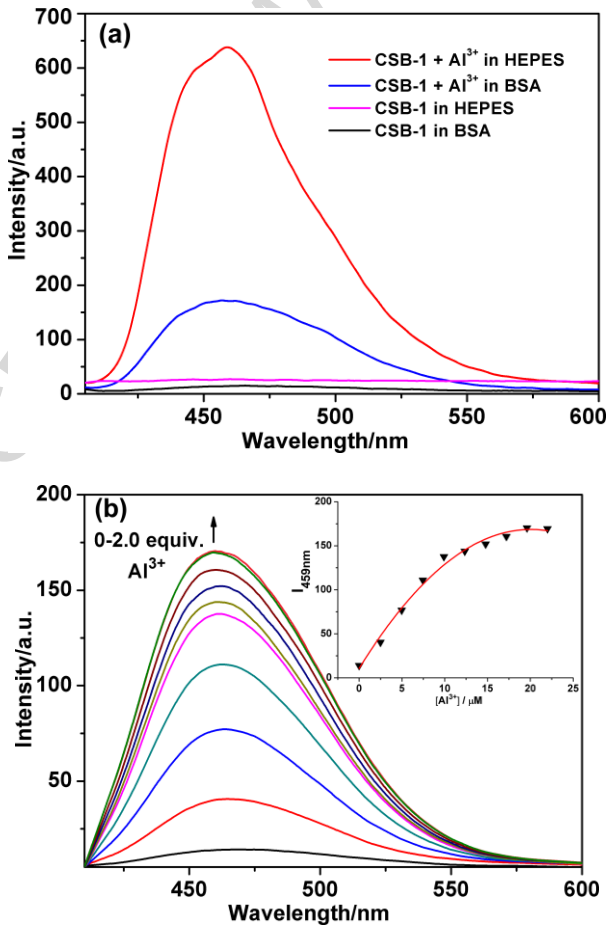


**Figure 5**. (a) Fluorescence detection of $Al^{3+}$ in mixed HEPES buffer (pH 7.4) and BSA medium. (b) Fluorescence titration of **CSB-1** (10 μM) with $Al^{3+}$ (0-20 μM) in BSA medium. (*inset*) plot of fluorescence intensity at 459 nm as a function of $Al^{3+}$ concentration.

of the **CSB-1** at 461 nm is enhanced by ~24 fold upon addition of 5 equiv. of $Al^{3+}$. The fluorescence titration with $Al^{3+}$ in BSA medium reveals a gradual blue shift of the emission band to 459 nm and a concomitant intensity enhancement. No significant enhancement is observed after addition of 2.0 equiv. of $Al^{3+}$ (Figure 5b). The plot of the emission intensity at 459 nm *vs* concentration of $Al^{3+}$ shows linearity at low concentration and supports that $Al^{3+}$ quantification is possible in BSA medium particularly, assessing the presence of $Al^{3+}$ in blood plasma (Figure 5b inset).

### *3.1.3 Evidence for $Al^{3+}$ binding*

To gain insight into the interaction between **CSB-1** and $Al^{3+}$, $^1$H NMR titration experiment was carried out in DMSO-$d_6$ (Figure 6). After the addition of only 0.5 equiv. of $Al^{3+}$, the signals of the hydroxyl protons of the free **CSB-1** at $\delta$ (ppm) = 15.66 disappeared completely due to the instantaneous deprotonation of the phenolic -OH groups and the coordination of **CSB-1** with $Al^{3+}$. The imine proton, $H_{11}$ of **CSB-1** is highly affected during the complexation process of **CSB-1** with metal ions and shows a gradual upfield shift from $\delta$ (ppm) = 9.97 to 9.62 upon addition of increasing amounts of $Al^{3+}$ (0 - 2 equiv.). The $^1$H NMR titration result supported the binding of $Al^{3+}$ with **CSB-1** through a chelation reaction *via* phenolic -O and the imine -N atoms.

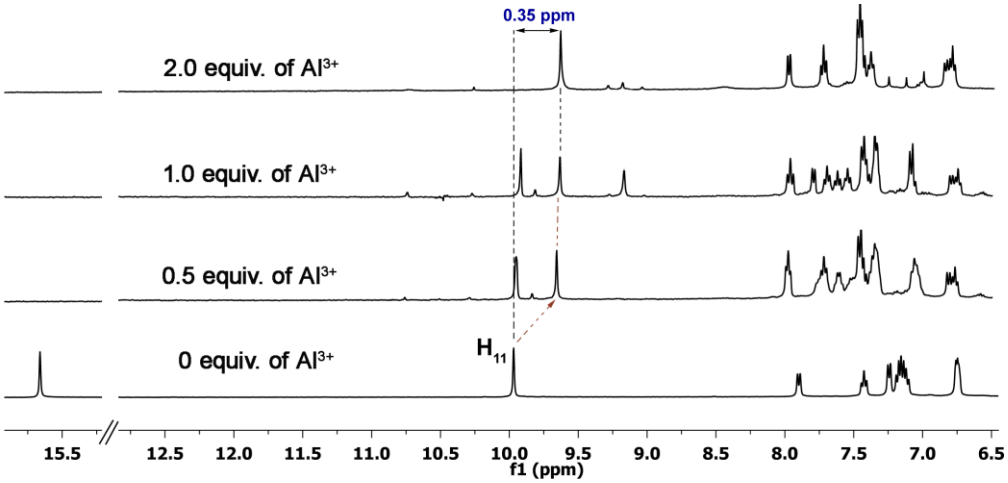


**Figure 6.** $^1$H NMR titration of **CSB-1** with $Al^{3+}$ in DMSO-$d_6$.

The ESI-MS spectrum clearly indicated the formation of the $Al^{3+}$-**CSB-1** complex upon treatment of **CSB-1** with excess $Al^{3+}$. A major peak is observed at *m/z* = 338.20 corresponding to the $[Al(\textbf{CSB-1})(MeOH)]^{+}$. The other peak is observed at *m/z* 306.15 indicating to the $[Al(\textbf{CSB-1})]^{+}$ and thereby confirming 1:1 stoichiometry of **CSB-1** to $Al^{3+}$ binding (Figure S7 in SI).

### *3.2 Probable binding mode and DFT study*

To further understand the electronic structure of the **CSB-1** and the $Al^{3+}$-**CSB-1** complex, we carried out density functional theory (DFT) calculations using the B3LYP/6-31G+ (d, p) basis set in the *Gaussian 03* program. The ESI-MS studies confirms that a solvent methanol is coordinated with the $Al^{3+}$-**CSB-1** complex. The formation of tetra coordinated Aluminum complex except for Al-salen complex is quite unusual, so it expected that a water molecule is also coordinated to the Aluminum in $Al^{3+}$-**CSB-1** complex as a fifth ligand. In the figure 7, the energy minimized structure and highest occupied molecular orbital (HOMO) and the lowest unoccupied molecular orbital (LUMO) of the **CSB-1** and the $Al^{3+}$-**CSB-1** complex is shown. The optimized structure of the $Al^{3+}$-**CSB-1** complex clearly shows that the central $Al^{3+}$ adopts a distorted square pyramidal geometry with an axial aqua ligand. Both the HOMO and LUMO is stabilized after the complex formation. The HOMO to LUMO energy gap in the free **CSB-1** ($\Delta E$ = 3.63 eV) is lowered considerably upon the $Al^{3+}$-**CSB-1** complex ($\Delta E$ = 2.28 eV) complex formation. The DFT calculation shows that the total energy of **CSB-1** ($E_{\textbf{CSB-1}}$ = -26451.40 eV) is significantly higher than the formed $Al^{3+}$-**CSB-1** complex ($E_{Al^{3+}\text{-}\textbf{CSB-1}}$ = -38244.84 eV) which suggests the higher stability of the $Al^{3+}$-**CSB-1** complex than the free **CSB-1**.

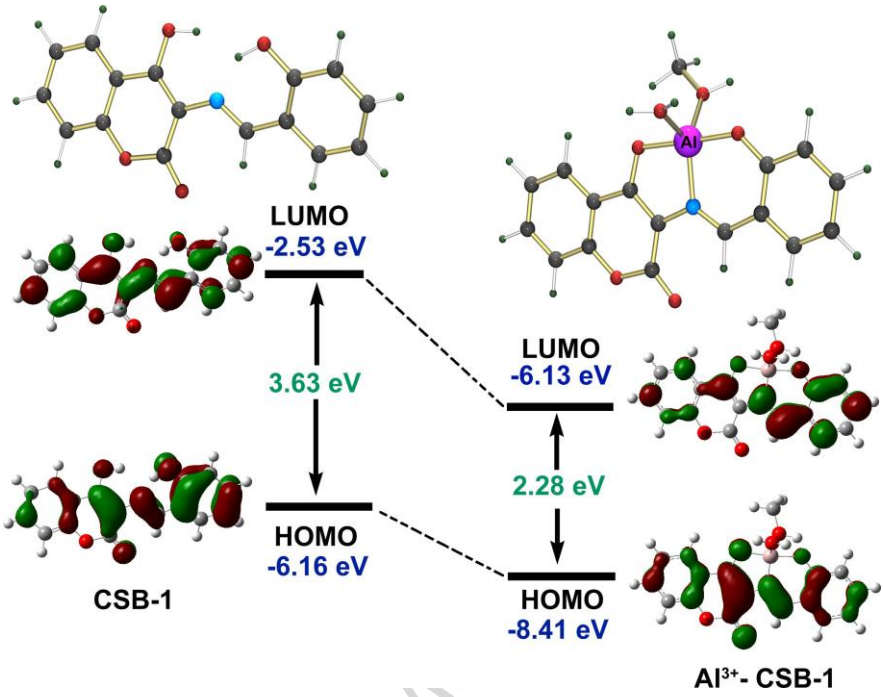


**Figure 7**. Energy optimized structure of (*left*) **CSB-1** and (*right*) [$Al^{3+}$-**CSB-1**] and the corresponding molecular orbital of **CSB-1** and [$Al^{3+}$-**CSB-1**].

### *3.3 Live cell imaging*

Due to the high selectivity and sensitivity of **CSB-1** toward $Al^{3+}$ in the mixed aqueous buffer, we further tried to find out the biological activity of our compound. Therefore, the living cell imaging experiment was done in HeLa cell using **CSB-1** for monitoring $Al^{3+}$ ions in biological systems. Using the fluorescence microscopy, an imaging application of **CSB-1** for $Al^{3+}$ in biological samples was developed. As shown in figure 8, the intracellular imaging performances of **CSB-1** on HeLa cells with the help of fluorescence microscopy displayed no significant intracellular fluorescence when treated with only 10 μM of **CSB-1** (Figure 8a and 8d) and incubated for 20 min at 37°C. In contrast, cells which were treated with both the $Al^{3+}$ (30 μM) and **CSB-1**, a bright blue intracellular fluorescence was observed without celluar alteration of morphology (Figure 8b and 8e) after 20 mins incubation. The bright blue fluorescence image of live HeLa cells indicates that the **CSB-1** pass through the cell

membrane, diffuse well within the cell and form stable complex with added $Al^{3+}$. Thus, above results clearly documents the applicability of **CSB-1** as a fluorescent chemosensor to detect intracellular $Al^{3+}$ ions by fluorescence OFF-ON mechanism.

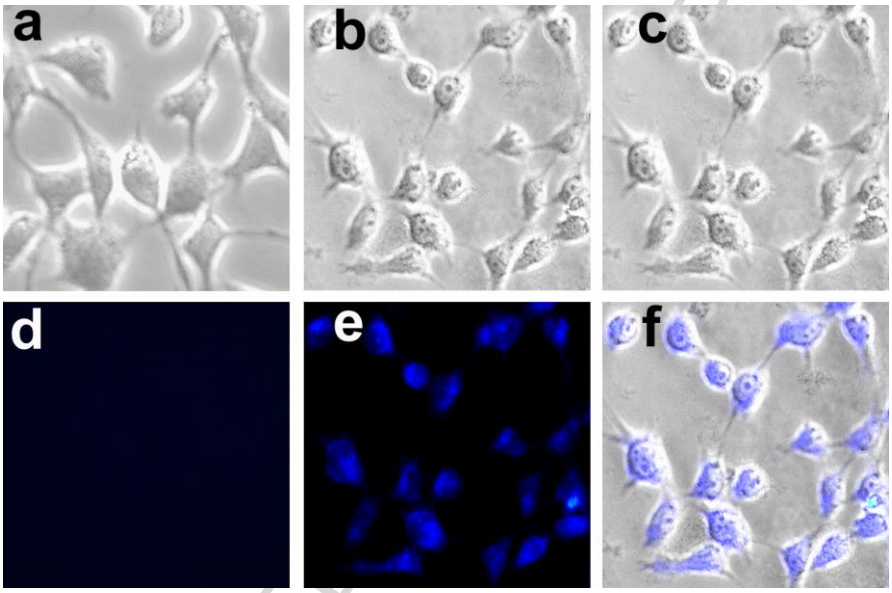


**Figure 8:** Images of HeLa cells: (a) bright field image of HeLa cells incubated with **CSB-1** (10 μM) for 20 min; (d) fluorescence image of (a); (b and c) bright field image of HeLa cells incubated with $Al^{3+}$ (30 μM) for 10 min. and the **CSB-1** (10 μM) for additional 10 min; (e) fluorescence image of (b) and (f) overlay image of (c) and (e).

## 4. Conclusions

We have successfully developed a new Schiff base compound, **CSB-1** from 3-amino-4-hydroxy-2H-chromen-2-one and salicylaldehyde to detect $Al^{3+}$ ion based on the chelation enhance fluorescence (CHEF) in mixed aqueous buffer media. Fluorescence intensity enhancement of 24-fold upon addition of 50 μM $Al^{3+}$ to **CSB-1** (10 μM) is observed. The possible fluorescent species of **CSB-1** with $Al^{3+}$ were deduced according to the ESI-MS and $^1H$ NMR spectroscopy. The probable working mechanism is based on the $Al^{3+}$-induced formation of a 1 : 1 $Al^{3+}$-**CSB-1** complex, which inhibits the C=N isomerization process and produces a chelation-enhanced fluorescence (CHEF) effect. The fluorescence "Turn–on"

sensing phenomenon caused by $Al^{3+}$ is irreversible and the formed $Al^{3+}$**-CSB-1** complex is highly stable which is supported by fluorescence spectroscopy and DFT study. The detection limits for $Al^{3+}$ was found to be as low as 1.34 μM. More importantly the developed chemosensor can also detect $Al^{3+}$ in the intracellular region of live human cervical cancer cells.

**Acknowledgements**

We thank DST SERB (SB/FT/CS/115/2012) for the financial assistance and Sophisticated Analytical and Instrumentation Facility (SAIF), North Eastern Hill University for NMR and Mass data. B.S and S.K.S thank North Eastern Hill University and RGNF SC for their research fellowship respectively. Also we would like to thank the reviewers for their critical comments and suggestions.

**Supplementary Material**

Supplementary data (UV-vis, fluorescence, $^{1}H$, $^{13}C$ NMR and MS spectra of the synthesized compound) associated with this article can be found, in the online version.

**References and notes**

1. A. P. De Silva, H. Q. N. Gunaratne, T. Gunnlaugsson, A. J. M. Huxley, C. P. McCoy, J. T. Rademacher, T. E. Rice, Chem. Rev. 97 (1997) 1515.
2. L. Prodi, F. Bolletta, M. Montalti, N. Zaccheroni, Coord. Chem. Rev. 205 (2000) 59.
3. S. Lee, K. K. Y. Yuen, K. A. Jolliffe, J. Yoon, Chem. Soc. Rev. 44 (2015) 1749.
4. Y. Jeong, J. Yoon, Inorg. Chim. Acta 381 (2012) 2.
5. S. Khatua, D. Samanta, J. W. Bats, M. Schmittel, Inorg. Chem. 51 (2012) 7075.
6. B. Chowdhury, S. Khatua, R. Dutta, S. Chakraborty, P. Ghosh, Inorg. Chem. 53 (2014) 8061.

7. L. González, F. Zapata, A. Caballero, P. Molina, C. Ramírez de Arellano, I. Alkorta, J. Elguero, Chem. Eur. J. 22 (2016) 7533.

8. F. Zapata, L. Gonzalez, A. Caballero, I. Alkorta, J. Elguero, P. Molina, Chem. Eur. J. 21 (2015) 9797.

9. P. Sabater, F. Zapata, A. Caballero, I. Fernández, C. Ramírez de Arellano, P. Molina, J. Org. Chem. 81 (2016) 3790.

10. M. C. González, F. Otón, A. Espinosa, A. Tárraga, P. Molina, Org. Biomol. Chem. 13 (2015) 1429.

11. M. C. González, F. Otón, R. A. Orenes, A. Espinosa, A. Tárraga, P. Molina, Organometallics 33 (2014) 2837.

12. S. C. Burdette, G. K. Walkup, B. Spingler, R. Y. Tsien, S. J. Lippard, J. Am. Chem. Soc. 123 (2001) 7831.

13. E. Palomares, R. Vilar, J. R. Durrant, Chem. Commun. (2004), 362-363.

14. M. Santra, B. Roy, K. H. Ahn, Org. Lett. 13 (2011) 3422.

15. A. S. Rao, D. Kim, T. Wang, K. H. Kim, S. Hwang, K. H. Ahn, Org. Lett. 14 (2012) 2598.

16. S. Khatua, M. Schmittel, Org. Lett. 15(17) (2013) 4422.

17. N. D. Priest, R. J. Talbot, D. Newton, J. P. Day, S. J. King, L. K. Fifield, Hum. Exp. Toxicol. 17 (1988) 296.

18. D. Krewski, R. A. Yokel, E. Nieboer, D. Borchelt, J. Cohen, J. Harry, S. Kacew, J. Lindsay, A. M. Mahfouz, V. Rondeau, J. Toxicol. Environ. Health, Part B 10 (2007) 1.

19. C. Exley, Environ. Sci. Process Impacts 15 (2013) 1807.

20. D. L. Godbold, E. Fritz, A. Huttermann, Proc. Natl. Acad. Sci. U. S. A. 85 (1988) 3888.

21. N. E. W. Alstad, B. M. Kjelsberg, L. A. Vøllestad, E. Lydersen, A. B. S. Poléo, Environ. Pollut. 133 (2005) 333.

22. J. Ren, H. Tian, Sensors 7 (2007) 3166.

23. G. D. Fasman, Coord. Chem. Rev. 149 (1996) 125.

24. A. Salifoglou, Coord. Chem. Rev. 228 (2002) 297.

25. J. Q. Wang, L. Huang, L. Gao, J. H. Zhu, Y. Wang, X. Fan, Z. Zou, Inorg. Chem. Commun. 11 (2008) 203.

26. D. Maity, T. Govindaraju, Inorg. Chem. 49 (2010) 7229.

27. G. Aragay, J. Pons, A. Merkoc, Chem. Rev. 111 (2011) 3433.

28. F. K. Hau, X. M. He, W. H. Lam, V. W. W. Yam, Chem. Commun. 47 (2011) 8778.

29. B. K. Datta, S. Mukherjee, C. Kar, A. Ramesh and G. Das, Anal. Chem. 85 (2013) 8369.

30. C. Kar, M. D. Adhikari, A. Ramesh, G. Das, Inorg. Chem. 52 (2013) 743.

31. K. Soroka, R. S. Vithanage, D. A. Phillips, B. Walker, P. K. Dasgupta, Anal. Chem. 59 (1987) 629.

32. J. L. Ren, J. Zhang, J. Qing Luo, X. K. Pei, Z. Xi Jiang, Analyst. 126 (2001) 698.

33. S. M. Ng, R. Narayanaswamy, Anal. Bioanal. Chem. 386 (2006) 1235.

34. Y. Zhao, Z. Lin, H. Liao, C. Duan, Q. Meng, Inorg. Chem. Commun. 9 (2006) 966.

35. L. Peng, Z. J. Zhou, X. Y. Wang, R. R. Wei, K. Li, Y. Xiang, A. J. Tong, Anal. Chim. Acta. 829 (2014) 54.

36. S. M. Z. Al-Kindy, F. E. O. Suliman, A. E. Pillay, Instrum. Sci. Technol. 34 (2006) 619.

37. A. Sahana, A. Benerjee, S. Lohar, A. Banik, S. K. Mukhopadhyay, D. A. Safin, M. G. Babashkina, M. Bolte, Y. Garcia, D. Das, Dalton Trans. 42 (2013) 13311.

38. Y. W. Choi, J. J. Lee, E. Nam, M. H. Lim, C. Kim, Tetrahedron, 72 (2016) 1998.

39. D. Maity, T. Govindaraju, Chem. Commun. 46 (2010) 4499.

40. T. J. Jia, W. Cao, X. J. Zheng, L. P. Jin, Tetrahedron Lett. 54 (2013) 3471.

41. C. Liang, W. Bu, C. Li, G. Men, M. Deng, Y. Jiangyao, H. Sun, S. Jiang, Dalton Trans. 44 (2015) 11352.

42. W. Wang, Z. Mao, M. Wang, L. -J. Liu, D. W. J. Kwong, C. -H. Leung, D. -L. Ma, Chem. Commun. 52 (2016) 3611.

43. S. Khatua, S. H. Choi, J. Lee, J. O. Huh, Y. Do, D. G. Churchill, Inorg. Chem. 48 (2009) 1799.

44. S. Khatua, S. H. Choi, J. Lee, K. Kim, Y. Do, D. G. Churchill, Inorg. Chem. 48 (2009) 2993.

45. S. Khatua, K. Kim, J. Kang, J. O. Huh, C. S. Hong, D. G. Churchill, Eur. J. Inorg. Chem. (2009) 3266.

46. S. Khatua, J. Kang, D. G. Churchill, New J. Chem. 34 (2010) 1163.

47. J.-S. Wu, Wei-Min Liu, X.-Q. Zhuang, F. Wang, P.-F. Wang, S.-L. Tao, X.-H. Zhang, S.-K. Wu, S.-T. Lee, Org. Lett. 9 (2007) 33.

48. K. K. Upadhyay, A. Kumar, Org. Biomol. Chem. 8 (2010) 4892.

49. Z. X. Li, M. M. Yu, L. F. Zhang, M. Yu, J. X. Liu, L. H. Wei, H. Y. Zhang, Chem. Commun. 46 (2010) 7169.

50. S. R. Trenor, A. R. Shultz, B. J. Love, T. E. Long, Chem. Rev. 104 (2004) 3059.

51. J. B. Wang, X. F. Qian, J. N. Cui, J. Org. Chem. 71 (2006) 4308.

52. D. Ray, P. K. Bharadwaj, Inorg. Chem. 47 (2008) 2252.

53. M. Suresh, A. Das, Tetrahedron Lett. 50 (2009) 5808.

54. T. Li, R. Fang, B. Wang, Y. Shao, J. Liu, S. Zhang, Z. Yang, Dalton Trans. 43 (2014) 2741.

55. I. Brady, D. Leane, H. P. Hughes, R. J. Forster, T. E. Keyes, Dalton Trans. (2004) 334.

56. L. Porrès, A. Holland, L. O. Palsson, A. P. Monkman, C. Kemp, A. Beeby. J. Fluoresc. 16 (2006) 267.

57. C. Lee, W. Yang, R. G. Parr, Phys. Rev. B 37 (1988) 785.

58. D. Andrae, U. Haeussermann, M. Dolg, H. Stoll, H. Preuss, Theor. Chim. Acta. 77 (1990) 123.

59. A. D. Becke, J. Chem. Phys. 98 (1993) 5648.

60. K. B. Kim, H. Kim, E. J. Song, S. Kim, I. Noh, C. Kim, Dalton Trans. 42 (2013) 16569.

61. A. K. Mandal, M. Suresh, P. Das, E. Suresh, M. Baidya, S. K. Ghosh, A. Das, Org. Lett. 14(12) (2012) 2980.

62. T. Han, X. Feng, B. Tong, J. Shi, L. Chen, J. Zhic, Y. Dong, Chem. Commun. 48 (2012) 416.

63. P. Ding, J. Wang, J. Cheng, Y. Zhao, Y. Ye, New J. Chem. 39 (2015) 342.

64. K. Ghosh, A. Majumdar, T. Sarkar, RSC Adv. 4 (2014) 23428.

65. Y-S. Mi, D-M. Liang, Y-T. Chen, X-B Luo, J-N. Xiang, RSC Adv. 4 (2014) 42337.

66. S. Samanta, S. Goswami, Md. N. Hoque, A. Ramesh, G. Das, Chem. Commun. 50 (2014) 11833.

67. Y-W. Liu, C-H. Chen, A-T. Wu, Analyst, 137 (2012) 5201.

68. M. Hosseini, M. R. Ganjali, M. Tavakoli, P. Norouzi, F. Faridbod, H. Goldooz, A. Badiei, J. Fluoresc. 21 (2011) 1509.

69. X. Su, C. Zhang, X. J. Xiao, A. Q. Xu, Z. D. Xu, M. P. Zhao, Chem. Commun. 49 (2013) 798.

# Graphical abstract

# A Coumarin Based Schiff Base Probe for Selective Fluorescence Detection of $Al^{3+}$ and its Application in Live Cell Imaging

Bhaskar Sen,[a] Sanjoy Kumar. Sheet,[a] Romita Thounaojam,[b] Ramen Jamatia,[a] Amarta Kumar. Pal,[a] Kripamoy Aguan[b] and Snehadrinarayan Khatua[a,*]

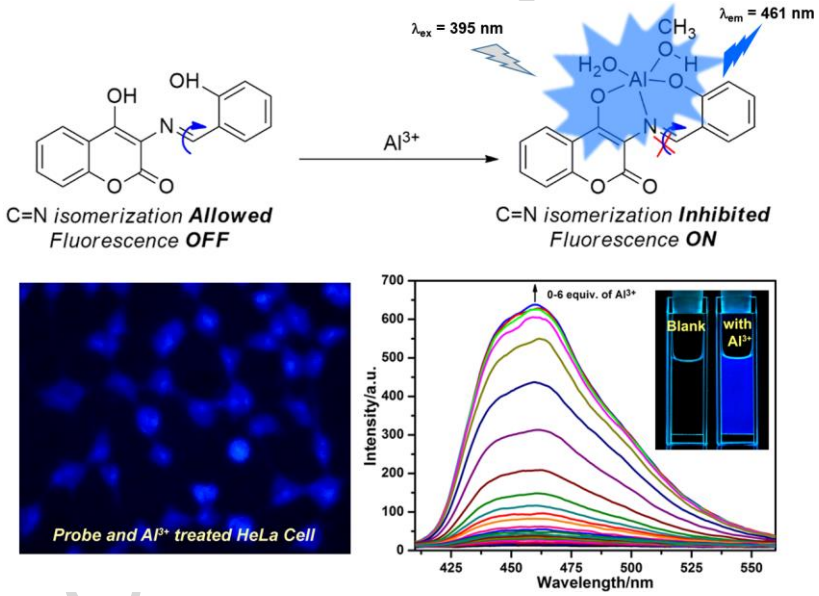

**Highlight**

- Fluorescence "Turn ON" $Al^{3+}$ sensing in mixed aqueous buffer solution based on CHEF effect is presented.
- The sensor is competent to quantify $Al^{3+}$ at its low concentration (detection limit = 1.34 μM).
- Compound diffuses well within the cell and appropriately detect the low amount extracellular $Al^{3+}$ ions.